Composite Structures 97 (2013) 30–39

Contents lists available at SciVerse ScienceDirect

Composite Structures

journal homepage: www.elsevier.com/locate/compstruct

# Shear-deformable thin-walled composite Beams in internal and external resonance

Sebastián P. Machado *, C. Martín Saravia

*Grupo Análisis de Sistemas Mecánicos, Centro de Investigaciones de Mecánica Teórica y Aplicada, Universidad Tecnológica Nacional FRBB, 11 de Abril 461, B8000LMI Bahía Blanca, Argentina*
*Consejo Nacional de Investigaciones Científicas y Tecnológicas, Argentina*

ARTICLE INFO

*Article history:*
Available online 7 November 2012

*Keywords:*
Shear flexibility
Internal resonance
Composite material
Thin-walled beams

ABSTRACT

The non-linear dynamic response of thin-walled composite beams is analyzed considering the effect of shear deformation. The model is based on a small strain and large rotation and displacements theory, which is formulated through the adoption of a higher-order displacement field and takes into account shear flexibility (bending and warping shear). The beam is assumed to be in internal resonance conditions of the kind 2:3:1, so that quadratic, cubic and combination resonances occur. In the analysis of a weakly nonlinear continuous system, the Galerkin's method is employed to express the problem in terms of generalized coordinates. Then, the perturbation method of multiple scales is applied to the reduced system in order to obtain the equations of amplitude and modulation. The equilibrium solution is governed by the modal coupling and experience a complex behavior composed by saddle–noddle and Hopf bifurcations. The results of the analysis show that the equilibrium solutions are influenced by the shear effect, when this effect is ignored the amplitude of vibration is reduced significantly, thus altering the dynamic response of the beam. This alteration can infer in an incorrect stability prediction of the periodic solutions.



## 1. Introduction

Structural members made of composites materials have been historically associated to aerospace industry and its very high performance requirements. For example, thin-walled beam structures made of advanced anisotropic composite materials are found in the design of the aircraft wings, helicopter blades, axles of vehicles and so on. It is due that fiber reinforced composite materials can be used to enhance the response characteristics of such structures that operate in complex environmental conditions. Nowadays, there is a new tendency to incorporate fiber reinforced plastic (FRP) in many kind of non-aerospace purpose, such in bridge design or automotive and others industrial applications. However, greater awareness and knowledge of FRP materials is still needed within the construction industry.

On the other hand, the effect of shear flexibility in this kind of materials is a phenomenon very important and crucial in some beam models. For example, it has been demonstrated the significance of this effect in linear and non-linear static analysis [1–5] and in linear dynamic cases [6,7]. Machado and Cortínez showed that shear-deformation effect may significantly decrease the buckling loads [1] and the values of the equilibrium path (post-buckling) [4]. They demonstrated that this effect is more significant when one of the material axes coincides with the beam axis and for short beams. The shear effect was also analyzed for different boundary conditions, determining a larger influence in clamped–clamped conditions [1]. On the other hand, the discard of shear deformation results in an overprediction of the resonance behavior, in the sense of the shift of the domain of instability toward larger excitation frequencies [6]. The influences of shear deformation and geometrically non-linear coupling on the dynamic stability of thin-walled laminated composite beam were analyzed by Machado and Cortínez [7]. They showed the influence of this effect on the unstable regions sizes, noting that the boundaries of instability move to the right when this effect is ignored.

We consider in the present article the influence of shear deformation effect on the non-linear response of a simply supported beam subjected to a primary resonant excitation of its first mode. The analysis accounts for a lateral load, modal damping and two fiber orientations. The second and third natural frequencies are approximately two and three times the first natural frequency, respectively. The flexural–torsional coupling produces a quadratic and cubic non-linearity in the governing non-linear partial–differential equation. Because of the quadratic and cubic non-linearity and the two-to-one and three-to-one ratio of the second and third with the first natural frequencies, the beam exhibits an internal (autoparametric) resonance that couples the first, second and third modes, resulting in energy exchange between them. For a comprehensive review of

* Corresponding author. Tel.: +54 291 4555220; fax: +54 291 4555311.
*E-mail addresses:* smachado@frbb.utn.edu.ar (S.P. Machado), msaravia@frbb.utn.edu.ar (C. Martín Saravia).

0263-8223/$ - see front matter © 2012 Elsevier Ltd. All rights reserved.
http://dx.doi.org/10.1016/j.compstruct.2012.10.018

non-linear modal interactions we refer the reader to References [9,10].

In this paper we present a brief review of some of the studies of the response of systems exhibiting two-to-one and three-to-one internal resonances to primary resonant excitations. Crespo da Silva and Glynn [11,12] developed a non-linear shear-undeformable beam model with a compact cross-section and derived a set of integro-partial–differential equations governing flexural–flexural–torsional motions of inextensional beams, including geometric and inertia non-linearities. They used these equations and the method of multiple scales to ascertain the importance of the geometric terms [12], it was concluded that they cannot be neglected for the lower modes, especially the first mode. Luongo et al. [13] and Crespo da Silva and Zaretzky [14] analyzed shear and axial undeformable beams. In the last reference the flexural–torsional free motions are studied for a cantilever beam, having close bending and torsional frequencies; although beams with non-compact cross-section are considered, the warping effects are neglected. In these articles a non-linear one-dimensional polar model of compact beam is derived, it is capable of studying interactions between flexural and torsional motions occurring in beam-like structures in several internal resonance conditions. Recently, Fonseca and Ribeiro [15] analyzed the non-linear planar motions and the non-linear resonance frequencies by means of a *p*-version finite element formulated for geometrically non-linear vibrations. This work was continued by Lopes Alonso and Ribeiro [16] investigating the free vibrations of clamped–clamped circular cross section beams using hierarchic sets of displacement shape functions and that simultaneously considers bending, torsion and longitudinal deformation. They employed the harmonic balance method to show the variation of the bending and torsional shapes of vibration with the non-linear natural frequency. Besides they found internal resonances in bending and torsion. Stoykov and Ribeiro [17] extended their model to investigate the effects of the warping function, longitudinal displacements of second order and shear deformations on the non-linear bending-torsion vibrations of rectangular cross section. The effect of the shear deformation on the amplitude-frequency response curves was shown by Luo et al. [18]. They used the incremental harmonic balance method to study the response of a composite beam with clamping of two ends. In relation to thin-walled beams, Di Egidio et al. [19,20] presented the dynamic response of an open cross-section beam divided in two works. In the first part [19] they developed a shear undeformable thin-walled beam, where the effects of non-linear in-plane and out-of-plane warping and torsional elongation were included in the model. This model was used in the second part [20] to study the dynamic coupling phenomena in conditions of internal resonance. In spite of the practical interest and future potential of the composite beam structures, particularly in the context of aerospace and mechanical applications, there are no investigations about the non-linear dynamic response of thin-walled composite beams considering the effect of shear deformation.

The purpose of this paper is to study the influence of shear deformation on the three dimensional large amplitude oscillations of thin-walled composite beams. The analysis is based on a beam model previously developed by the authors [1,4] which is formulated in the context of small strain and large rotation and displacements theory, through the adoption of a shear-deformable displacement field (accounting for bending and warping shear), considering a laminate stacking sequence symmetric and balanced. Machado and Cortínez [7,8] investigated the effect of non-linearity degree considered in their formulation. They analyzed analytically and numerically the effect of approximations on a geometrically non-linear beam theory on the stability and free vibration behavior of thin-walled composite beams. Machado [8] demonstrated that second order approximation, which is very much used in finite element models, produces the loss of some terms corresponding to the flexural–torsional coupling in the non-linear strains. In order to perform the non-linear dynamic analysis, the Galerkin procedure is used to obtain a discrete form of the equations of motion. Multiple time scales method is used to obtain modulation-phase equations [21] and the reconstitution method proposed in [22] is adopted to return to the true time domain. Steady-state solutions and their stability are studied by using the model proposed. For principal external resonance of the first mode, the influence of internal resonance is illustrated in frequency–response plots. The system is shown to have Hopf bifurcations and saddle node bifurcations for different parameter values. The influence of the shear deformation effect on the equilibrium solutions is illustrated. It is found that the vibration amplitude is reduced significantly when this effect is ignored, altering the dynamic response of the beam. This alteration can conclude in an incorrect stability prediction of the periodic solutions.

## 2. Kinematics

Consider a straight thin-walled composite beam with an arbitrary cross-section (Fig. 1). The points of the structural member are referred to a Cartesian co-ordinate system $(x,\bar{y},\bar{z})$, where the $x$-axis is parallel to the longitudinal axis of the beam while $\bar{y}$ and $\bar{z}$ are the principal axes of the cross-section. The axes $y$ and $z$ are parallel to the principal ones but having their origin at the shear center (defined according to Vlasov's theory of isotropic beams). The co-ordinates corresponding to points lying on the middle line are denoted as $Y$ and $Z$ (or $\overline{Y}$ and $\overline{Z}$). In addition, a circumferential co-ordinate $s$ and a normal co-ordinate $n$ are introduced on the middle contour of the cross-section.

$$\bar{y}(s,n) = \overline{Y}(s) - n\frac{dZ}{ds}, \quad \bar{z}(s,n) = \overline{Z}(s) + n\frac{dY}{ds} \tag{1}$$

$$y(s,n) = Y(s) - n\frac{dZ}{ds}, \quad z(s,n) = Z(s) + n\frac{dY}{ds}. \tag{2}$$

On the other hand, $y_0$ and $z_0$ are the centroidal co-ordinates measured with respect to the shear center.

$$\bar{y}(s,n) = y(s,n) - y_0, \bar{z}(s,n) = z(s,n) - z_0. \tag{3}$$

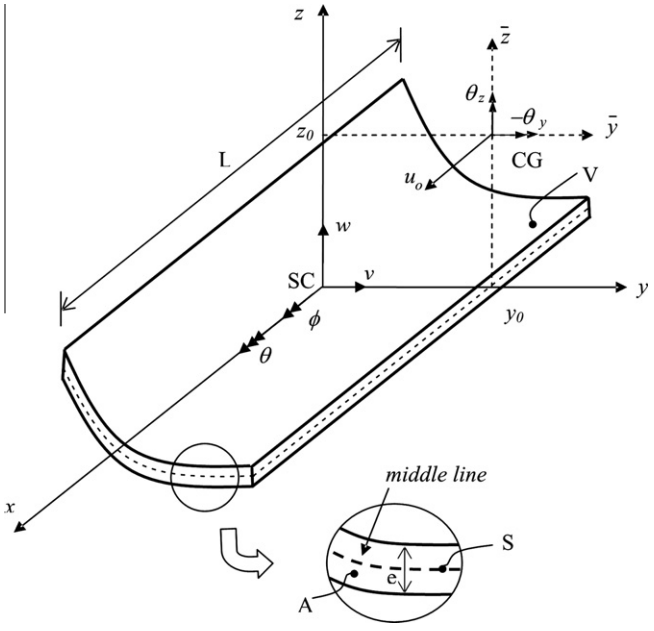


**Fig. 1.** Co-ordinate system of the cross-section and notation for displacement measures.

The present structural model is based on the following assumptions [4]:

(1) The cross-section contour is rigid in its own plane.
(2) The warping distribution is assumed to be given by the Saint–Venant function for isotropic beams.
(3) Flexural rotations (about the $\bar{y}$ and $\bar{z}$ axes) are assumed to be moderate, while the twist $\phi$ of the cross-section can be arbitrarily large.
(4) Shell force and moment resultants corresponding to the circumferential stress $\sigma_{ss}$ and the force resultant corresponding to $\gamma_{ns}$ are neglected.
(5) The curvature at any point of the shell is neglected.
(6) Twisting linear curvature of the shell is expressed according to the classical plate theory.
(7) The laminate stacking sequence is assumed to be symmetric and balanced [23].

According to these hypotheses the displacement field is assumed to be:

$$\begin{aligned} u_x &= u_o - \bar{y}(\theta_z\cos\phi - \theta_y\sin\phi) - \bar{z}(\theta_y\cos\phi - \theta_z\sin\phi) \\ &\quad + \omega\left[\theta - \frac{1}{2}\left(\theta'_y\theta_z - \theta_y\theta'_z\right)\right] + (\theta_z z_0 - \theta_y y_0)\sin\phi, \\ u_y &= v - z\sin\phi - y(1-\cos\phi) - \frac{1}{2}\left(\theta_z^2\bar{y} + \theta_z\theta_y\bar{z}\right), \\ u_z &= w + y\sin\phi - z(1-\cos\phi) - \frac{1}{2}\left(\theta_y^2\bar{z} + \theta_z\theta_y\bar{y}\right). \end{aligned} \tag{4}$$

This expression is a generalization of others previously proposed in the literature as explained for Machado and Cortínez [4]. To analyze the influence of shear flexibility on the non-linear dynamic behavior this effect can be neglected considering $\theta_z = v'$, $\theta_y = w'$ and $\theta = \phi'$. Moreover, the displacement field of the classical Vlasov theory is obtained when non-linear effects are ignored. In the above expressions $\phi$, $\theta_y$ and $\theta_z$ are measures of the rotations about the shear center axis, $\bar{y}$ and $\bar{z}$ axes, respectively. The variable $\theta$ is a measure of the torsional warping along the beam and in the present formulation is an independent variable. Furthermore the superscript 'prime' denotes derivation with respect to the variable $x$.

The warping function $\omega$ of the thin-walled cross-section may be defined as:

$$\omega(s,n) = \omega_p(s) + \omega_s(s,n), \tag{5}$$

where $\omega_p$ and $\omega_s$ are the contour warping function and the thickness warping function, respectively. They are defined in the form [4]:

$$\begin{aligned} \omega_p(s) &= \frac{1}{S}\left[\int_0^S\left(\int_{s_0}^s [r(\sigma) - \psi(\sigma)]d\sigma\right)ds\right] - \int_{s_0}^s [r(\sigma) - \psi(\sigma)]d\sigma, \\ \omega_s(s,n) &= -nl(s), \end{aligned} \tag{6a, b}$$

where $\sigma$ is a dummy variable, and

$$r(s) = -Z(s)\frac{dY}{ds} + Y(s)\frac{dZ}{ds}, \tag{7}$$

$$l(s) = Y(s)\frac{dY}{ds} + Z(s)\frac{dZ}{ds}, \tag{8}$$

$r(s)$ represents the perpendicular distance from the shear center to the tangent at any point of the mid-surface contour, and $l(s)$ represents the perpendicular distance from the shear center to the normal at any point of the mid-surface contour.

In Eq. (6a) $\psi$ is the shear strain at the middle line, obtained by means of the Saint–Venant theory of pure torsion for isotropic beams and normalized with respect to $d\phi/dx$ [4]. For the case of open sections $\psi = 0$.

## 3. The strain field

The displacements with respect to the curvilinear system $(x,s,n)$ are obtained by means of the following expressions:

$$\overline{U} = u_x(x,s,n), \tag{9}$$

$$\overline{V} = u_y(x,s,n)\frac{dY}{ds} + u_z(x,s,n)\frac{dZ}{ds}, \tag{10}$$

$$\overline{W} = -u_y(x,s,n)\frac{dZ}{ds} + u_z(x,s,n)\frac{dY}{ds}. \tag{11}$$

The three non-zero components $\varepsilon_{xx}$, $\varepsilon_{xs}$, $\varepsilon_{xn}$ of the Green's strain tensor are given by:

$$\varepsilon_{xx} = \frac{\partial\overline{U}}{\partial x} + \frac{1}{2}\left[\left(\frac{\partial\overline{U}}{\partial x}\right)^2 + \left(\frac{\partial\overline{V}}{\partial x}\right)^2 + \left(\frac{\partial\overline{W}}{\partial x}\right)^2\right], \tag{12}$$

$$\varepsilon_{xs} = \frac{1}{2}\left[\frac{\partial\overline{U}}{\partial s} + \frac{\partial\overline{V}}{\partial x} + \frac{\partial\overline{U}}{\partial x}\frac{\partial\overline{U}}{\partial s} + \frac{\partial\overline{V}}{\partial x}\frac{\partial\overline{V}}{\partial s} + \frac{\partial\overline{W}}{\partial x}\frac{\partial\overline{W}}{\partial s}\right], \tag{13}$$

$$\varepsilon_{xn} = \frac{1}{2}\left[\frac{\partial\overline{U}}{\partial n} + \frac{\partial\overline{W}}{\partial x} + \frac{\partial\overline{U}}{\partial x}\frac{\partial\overline{U}}{\partial n} + \frac{\partial\overline{V}}{\partial x}\frac{\partial\overline{V}}{\partial n} + \frac{\partial\overline{W}}{\partial x}\frac{\partial\overline{W}}{\partial n}\right]. \tag{14}$$

Substituting expressions Eq. (4) into Eqs. (9)–(11) and then into Eqs. (12)–(14), employing the relations Eqs. (1)–(3) and (5)–(8), after simplifying some higher order terms, the components of the strain tensor are expressed in the following form:

$$\begin{aligned} \varepsilon_{xx} &= \varepsilon_{xx}^{(0)} + n\kappa_{xx}^{(1)}, \quad \gamma_{xs} = 2\varepsilon_{xs} = \gamma_{xs}^{(0)} + n\kappa_{xs}^{(1)}, \quad \gamma_{xn} = 2\varepsilon_{xn} \\ &= \gamma_{xn}^{(0)}, \end{aligned} \tag{15}$$

where

$$\begin{aligned} \varepsilon_{xx}^{(0)} &= u'_o + \frac{1}{2}\left(v'^2 + w'^2\right) + \omega_p\left[\theta' - \frac{1}{2}\left(\theta_z\theta''_y - \theta_y\theta''_z\right)\right] \\ &\quad + \overline{Z}\left(-\theta'_y\cos\phi + \theta'_z\sin\phi\right) + \overline{Y}\left(-\theta'_z\cos\phi - \theta'_y\sin\phi\right) \\ &\quad + \frac{1}{2}\phi'^2(Y^2 + Z^2) + \left(z_0\theta'_z - y_0\theta'_y\right)\sin\phi + \phi'(z_0\theta_z - y_0\theta_y)\cos\phi, \end{aligned} \tag{16}$$

$$\begin{aligned} \kappa_{xx}^{(1)} &= -\frac{dZ}{ds}\left(-\theta'_z\cos\phi - \theta'_y\sin\phi\right) + \frac{dY}{ds}\left(-\theta'_y\cos\phi + \theta'_z\sin\phi\right) \\ &\quad - l\left[\theta' - \frac{1}{2}\left(\theta_z\theta''_y - \theta_y\theta''_z\right)\right] - r\phi'^2, \end{aligned} \tag{17}$$

$$\begin{aligned} \gamma_{xs}^{(0)} &= \frac{dY}{ds}\left[(v' - \theta_z)\cos\phi - z_0\frac{1}{2}\left(\theta_z\theta'_y - \theta_y\theta'_z\right) + (w' - \theta_y)\sin\phi\right] \\ &\quad + (r - \psi)(\phi' - \theta) + \frac{dZ}{ds}\left[(w' - \theta_y)\cos\phi + y_0\frac{1}{2}\left(\theta_z\theta'_y - \theta_y\theta'_z\right)\right. \\ &\quad \left.-(v' - \theta_z)\sin\phi\right] + \psi\left[\phi' - \frac{1}{2}\left(\theta_z\theta'_y - \theta_y\theta'_z\right)\right], \end{aligned} \tag{18}$$

$$\kappa_{xs}^{(1)} = -2\left[\phi' - \frac{1}{2}\left(\theta_z\theta'_y - \theta_y\theta'_z\right)\right], \tag{19}$$

$$\begin{aligned} \gamma_{xn}^{(0)} &= \frac{dY}{ds}\left[(w' - \theta_y)\cos\phi + y_0\frac{1}{2}\left(\theta_z\theta'_y - \theta_y\theta'_z\right) - (v' - \theta_z)\sin\phi\right] \\ &\quad - \frac{dZ}{ds}\left[(v' - \theta_z)\cos\phi - z_0\frac{1}{2}\left(\theta_z\theta'_y - \theta_y\theta'_z\right) + (w' - \theta_y)\sin\phi\right] \\ &\quad + l(\phi' - \theta). \end{aligned} \tag{20}$$

## 4. Variational formulation

Taking into account the adopted assumptions, the principle of virtual work for a composite shell may be expressed in the form [7]:

$$\int\int (N_{xx}\delta\varepsilon_{xx}^{(0)} + M_{xx}\delta\kappa_{xx}^{(1)} + N_{xs}\delta\gamma_{xs}^{(0)} + M_{xs}\delta\kappa_{xs}^{(1)} + N_{xn}\delta\gamma_{xn}^{(0)})ds\,dx - \iiint \rho(\ddot{u}_x\delta u_x + \ddot{u}_y\delta u_y + \ddot{u}_z\delta u_z)ds\,dn\,dx - \int\int (\bar{q}_x\delta\bar{u}_x + \bar{q}_y\delta\bar{u}_y + \bar{q}_z\delta\bar{u}_z)ds\,dx - \int\int (\bar{p}_x\delta u_x + \bar{p}_y\delta u_y + \bar{p}_z\delta u_z)\big|_{x=0}ds\,dn - \int\int (\bar{p}_x\delta u_x + \bar{p}_y\delta u_y + \bar{p}_z\delta u_z)\big|_{x=L}ds dn - \iiint (\bar{f}_x\delta u_x + \bar{f}_y\delta u_y + \bar{f}_z\delta u_z)ds\,dn\,dx = 0, \tag{21}$$

where $N_{xx}$, $N_{xs}$, $M_{xx}$, $M_{xs}$ and $N_{xn}$ are the shell stress resultants. The beam is subjected to wall surface tractions $\bar{q}_x$, $\bar{q}_y$ and $\bar{q}_z$ specified per unit area of the undeformed middle surface and acting along the $x$, $y$ and $z$ directions, respectively. Similarly, $\bar{p}_x$, $\bar{p}_y$ and $\bar{p}_z$ are the end tractions per unit area of the undeformed cross-section specified at $x = 0$ and $x = L$, where $L$ is the undeformed length of the beam. Besides, $\bar{f}_x$, $\bar{f}_y$ and $\bar{f}_z$ are the body forces per unit of volume. Finally, $\bar{u}_x$, $\bar{u}_y$ and $\bar{u}_z$ denote displacements at the middle line.

## 5. Constitutive equations

The constitutive equations of symmetrically balanced laminates may be expressed in the terms of shell stress resultants in the following form [23]:

$$\begin{Bmatrix} N_{xx} \\ N_{xs} \\ N_{xn} \\ M_{xx} \\ M_{xs} \end{Bmatrix} = \begin{bmatrix} \overline{A}_{11} & 0 & 0 & 0 & 0 \\ 0 & \overline{A}_{66} & 0 & 0 & 0 \\ 0 & 0 & \overline{A}_{55}^{(H)} & 0 & 0 \\ 0 & 0 & 0 & \overline{D}_{11} & 0 \\ 0 & 0 & 0 & 0 & \overline{D}_{66} \end{bmatrix} \begin{Bmatrix} \varepsilon_{xx}^{(0)} \\ \gamma_{xs}^{(0)} \\ \gamma_{xn}^{(0)} \\ \kappa_{xx}^{(1)} \\ \kappa_{xs}^{(1)} \end{Bmatrix}, \tag{22}$$

with

$$\overline{A}_{11} = A_{11} - \frac{A_{12}^2}{A_{22}}, \quad \overline{A}_{66} = A_{66} - \frac{A_{26}^2}{A_{22}}, \quad \overline{A}_{55}^{(H)} = A_{55}^{(H)} - \frac{\left(A_{45}^{(H)}\right)^2}{A_{44}^{(H)}},$$
$$\overline{D}_{11} = D_{11} - \frac{D_{12}^2}{D_{22}}, \quad \overline{D}_{66} = D_{66} - \frac{D_{26}^2}{D_{22}}, \tag{23}$$

where $A_{ij}$, $D_{ij}$ and $A_{ij}^{(H)}$ are plate stiffness coefficients defined according to the lamination theory presented by Barbero [23]. The coefficient $\overline{D}_{16}$ has been neglected because of its low value for the considered laminate stacking sequence.

## 6. Principle of virtual work for thin-walled beams

Substituting the kinematics expressions and the constitutive equations Eq. (22) into Eq. (21) and integrating with respect to $s$, one obtains the one-dimensional expression for the virtual work equation given by:

$$L_M + L_K + L_P = 0, \tag{24}$$

where $L_M$, $L_k$ and $L_p$ represent the virtual work contributions due to the inertial, internal and external forces, respectively. The expression $L_M$ is:

$$L_M = \int_0^L \rho\left[A\frac{\partial^2 u_0}{\partial t^2}\delta u_0 + I_z\frac{\partial^2\theta_z}{\partial t^2}\delta\theta_z + I_y\frac{\partial^2\theta_y}{\partial t^2}\delta\theta_y + C_w\frac{\partial^2\theta}{\partial t^2}\delta\theta + A\frac{\partial^2}{\partial t^2}(v - z_0\phi)\delta v + A\frac{\partial^2}{\partial t^2}(w + y_0\phi)\delta w + \frac{\partial^2}{\partial t^2}(-Az_0 v + Ay_0 w + I_s\phi)\delta\phi\right]dx, \tag{25}$$

where $A$ is the cross-sectional area, $I_z$ and $I_y$ are the principal moments of inertia of the cross-section, $C_w$ is the warping constant, $I_s$ is the polar moment with respect to the shear center and $\rho$ is the mean density of the laminate.

The expressions of $L_k$ and $L_p$ are the same as presented by Machado and Cortínez in [4]; in the same way, the 1-D beam forces in terms of the shell forces, have been defined in this last reference. Although the $L_k$ expressions were already presented for the first author in [4], the same ones are included here again to give an idea of the complexity or size of the equations.

$$\begin{aligned} L_K = \int_0^L \Big\{ & \delta u_0'\Big[N + u_0'N - M_z\left(\theta_z'\cos\phi + \theta_y'\ \text{sen}\ \phi\right) - M_y\left(\theta_y'\cos\phi + \theta_z'\ \text{sen}\ \phi\right) - Q_y(\theta_z\cos\phi + \theta_y\ \text{sen}\ \phi) - Q_z(\theta_y\cos\phi + \theta_z\ \text{sen}\ \phi)\Big] + \delta v'(Q_y\cos\phi - Q_z\ \text{sen}\ \phi + v'N) \\ & + \delta w'(Q_z\cos\phi + Q_y\ \text{sen}\ \phi + w'N) + \delta\theta_z\Big[-Q_y(1+u_0')\cos\phi + Q_z(1+u_0')\ \text{sen}\ \phi + \frac{1}{2}(Q_z y_0 - Q_y z_0)\theta_y' - \frac{1}{2}T_{sv}\theta_y' - \frac{1}{2}B\theta_y''\Big] \\ & + \delta\theta_z'\Big[-M_z(1+u_0')\cos\phi + M_y(1+u_0')\ \text{sen}\ \phi + Nz_0\ \text{sen}\ \phi + \frac{1}{2}(Q_y z_0 - Q_z y_0)\theta_y + \frac{1}{2}T_{sv}\theta_y + \theta_z'P_{zz} + \theta_y'P_{yz}\Big] \\ & + \delta\theta_y\Big[-Q_z(1+u_0')\cos\phi - Q_y(1+u_0')\ \text{sen}\ \phi + \frac{1}{2}(Q_y z_0 - Q_z y_0)\theta_z' + \frac{1}{2}T_{sv}\theta_z' + \frac{1}{2}B\theta_z''\Big] \\ & + \delta\theta_y'\Big[-M_y(1+u_0')\cos\phi - M_z(1+u_0')\ \text{sen}\ \phi - Ny_0\ \text{sen}\ \phi + \frac{1}{2}(Q_z y_0 - Q_y z_0)\theta_z - \frac{1}{2}T_{sv}\theta_z + \theta_z'P_{yz} + \theta_y'P_{yy}\Big] \\ & + \delta\phi\Big[M_y\Big(\left(\theta_y' + \theta_y'u_0'\right)\ \text{sen}\ \phi + \left(\theta_z' + \theta_z'u_0'\right)\cos\phi\Big) + M_z\Big(\left(\theta_z' + \theta_z'u_0'\right)\ \text{sen}\ \phi - \left(\theta_y' + \theta_y'u_0'\right)\cos\phi\Big) + Q_y((\theta_z - v' + \theta_z u_0')\text{sen}\phi - (\theta_y - w' + \theta_y u_0')\cos\phi) \\ & + N\left(z_0\theta_z' - y_0\theta_y'\right)\cos\phi + Q_z\left(\left(\theta_y - w' + \theta_y u_0'\right)\ \text{sen}\ \phi + (\theta_z - v' + \theta_z u_0')\cos\phi\right)\Big] + \delta\theta_z''\frac{1}{2}B\theta_y - \delta\theta_y''\frac{1}{2}B\theta_z + \delta\phi'[T_w + T_{sv} + B_1\phi'] + \delta\theta' B - \delta\theta T_w\Big\}dx. \end{aligned} \tag{26}$$

### 6.1. Discrete model

The equations of motion are discretized according to the Galerkin procedure. The independent displacements vector is expressed as a linear combination of given $x$-function vectors $\mathbf{f}_k(x) = \{f_{k1}(x), f_{k2}(x), f_{k3}(x)\}$ and unknown $t$-function coefficients $q_k(t)$:

$$\mathbf{u}(x,t) = \sum_{k=1}^{n} q_k(t)\mathbf{f}_k(x). \tag{27}$$

The functions $\mathbf{f}_k(x)$ are chosen as eigenfunctions of the linearized equations and boundary conditions. Since for a generic cross-section even the linear equations are coupled, all the components of $\mathbf{f}_k(x)$ are different from zero. By substituting Eq. (27) into Eq. (24) and vanishing separately terms in $\delta q_k$; 3n ordinary differential equations of motion follow. The linear natural frequencies of the beam depend on the boundary conditions and the sequence of lamination proposed in the analysis. For specific combinations of system parameters, the lower natural frequencies can be commensurable, leading to internal resonance in the system and non-linear interaction between the associated modes. We analyze the specific case of three mode interaction corresponding to particular system parameters. Two-and three-to-one internal resonances are considered in this study ($\omega_2 \cong 2\omega_1$ and $\omega_3 \cong 3\omega_1$). Since none of these first three modes is in internal resonance with any other

mode of the beam, all other modes except the directly or indirectly excited first, second or third mode decay with time due to the presence of damping and the first three modes will contribute to the long term system response [10]. Hence, by limiting the expansion Eq. (27) to $n = 3$ terms (e.g. by assuming a group of three modes with similar wave-length), three non-linear equations of the following type are obtained:

$$\ddot{q}_k + \omega_k^2 q_k = \sum_{i=1}^{n}\sum_{j=1}^{n} c_{kij} q_i q_j + \sum_{i=1}^{n}\sum_{j=1}^{n}\sum_{m=1}^{n} c_{kijm} q_i q_j q_m + f_k \ (k = 1,2,3,\ldots,n), \tag{28}$$

where $\omega_k$ is the $k$th linear frequency, $f_k$ the $k$th modal force, and $c_{kij}$ and $c_{kijm}$ are coefficients depending on the eigenfunctions. In the general case all quadratic and cubic terms appear in each equation of motion.

### 6.2. Amplitude and phase equations for the discrete model

A simply-supported beam with a monosymmetric cross-section, loaded by a concentrated harmonic force applied to the beam's centroid axis acting along the vertical section is considered, see Fig. 2. Using a three-mode discretization, the non-linear flexural–flexural–torsional oscillations are governed by the following three ordinary differential equations:

$$\begin{aligned}
&\ddot{q}_1 + d_1\dot{q}_1 + \omega_1^2 q_1 = c_1 q_1 q_2 + c_2 q_2 q_3 + c_3 q_1^3 + c_4 q_3^3 + c_5 q_1 q_2^2 + c_6 q_1 q_3^2 + c_7 q_3 q_1^2 + c_8 q_3 q_2^2 + c_{19} P,\\
&\ddot{q}_2 + d_2\dot{q}_2 + \omega_2^2 q_2 = c_9 q_1^2 + c_{10} q_2^2 + c_{11} q_3^2 + c_2 q_1 q_3 + c_{12} q_1 q_2 q_3 + c_{13} q_2^3 + c_5 q_2 q_1^2 + c_{14} q_2 q_3^2,\\
&\ddot{q}_3 + d_3\dot{q}_3 + \omega_3^2 q_3 = c_2 q_1 q_2 + c_{15} q_2 q_3 + c_{16} q_1^3 + c_{17} q_3^3 + c_8 q_1 q_2^2 + c_{18} q_1 q_3^2 + c_6 q_3 q_1^2 + c_{14} q_3 q_2^2 + c_{20} P,
\end{aligned} \tag{29}$$

where $q_i$ is the $i$th mode amplitude, $d_i$ are the modal damping coefficients and $P(t) = p\ e^{i\Omega t}$ is the load, of frequency $\Omega$ assumed to be in primary resonance with the $q_1$-mode. Moreover, the beam is assumed to be in internal resonance conditions of the kind 2:3:1, so that quadratic, cubic and combination resonances occur. The Eq. (29) is similar to those obtained by Di Egidio et al. [20]; the main difference is in the coefficients $c_i$ because the model used by them corresponds to a shear undeformable model valid for isotropic beams. The method of multiple time scales is employed to study the non-linear Eqs. (29); since non-linear terms are quadratic and cubic, a second-order expansion is developed. A small parameter $\varepsilon$ is introduced by ordering the linear damping and load amplitude as $d_i = \varepsilon^2\tilde{d}_i,\ p = \varepsilon^3\tilde{p}$. Moreover, the displacements $q_i$ are expanded as:

$$q_i(T_0,T_1,T_2,\varepsilon) = \varepsilon q_i^{(0)}(T_0,T_1,T_2,\varepsilon) + \varepsilon^2 q_i^{(1)}(T_0,T_1,T_2,\varepsilon) + \varepsilon^3 q_i^{(2)}(T_0,T_1,T_2,\varepsilon), \tag{30}$$

where $T_0 = t$, $T_1 = \varepsilon t$, $T_2 = \varepsilon^2 t$. $T_0$ is a fast scale, on which motions with frequencies of the order of $\Omega$ occur, while $T_1$ and $T_2$ are the slow scales, on which modulations of the amplitudes and phases take place.

Substituting Eq. (30) into Eqs. (29) and equating coefficients of like powers of $\varepsilon$, the following perturbation equations are obtained:

Order $\varepsilon$:

$$D_0^2 q_i^{(0)} + \omega_i^2 q_i^{(0)} = 0, \quad (i = 1,2,3). \tag{31}$$

Orden $\varepsilon^2$:

$$\begin{aligned}
D_0^2 q_1^{(1)} + \omega_1^2 q_1^{(1)} &= -2D_0D_1 q_1^{(0)} + c_1 q_1^{(0)} q_2^{(0)} + c_2 q_2^{(0)} q_3^{(0)},\\
D_0^2 q_2^{(1)} + \omega_2^2 q_2^{(1)} &= -2D_0D_1 q_2^{(0)} + c_9 q_1^{(0)^2} + c_{10} q_2^{(0)^2} + c_2 q_1^{(0)} q_3^{(0)} + c_{11} q_3^{(0)^2},\\
D_0^2 q_3^{(1)} + \omega_3^2 q_3^{(1)} &= -2D_0D_1 q_3^{(0)} + c_2 q_1^{(0)} q_2^{(0)} + c_{15} q_2^{(0)} q_3^{(0)}.
\end{aligned} \tag{32}$$

Orden $\varepsilon^3$:

$$\begin{aligned}
D_0^2 q_1^{(2)} + \omega_1^2 q_1^{(2)} = &-d_1 D_0 q_1^{(0)} - 2D_0D_1 q_1^{(1)} - D_1^2 q_1^{(0)} - 2D_0D_2 q_1^{(0)}\\
&+ c_3 q_1^{(0)^3} + c_1 q_1^{(1)} q_2^{(0)} + c_5 q_1^{(0)} q_2^{(0)^2} + c_1 q_1^{(0)} q_2^{(1)}\\
&+ c_7 q_1^{(0)^2} q_3^{(0)} + c_8 q_2^{(1)^2} q_3^{(0)} + c_2 q_2^{(1)} q_3^{(0)} + c_6 q_1^{(0)} q_3^{(0)^2}\\
&+ c_4 q_3^{(0)^3} + c_2 q_2^{(0)} q_3^{(1)} + c_{19} p e^{i\Omega T_0},
\end{aligned}$$

$$\begin{aligned}
D_0^2 q_2^{(2)} + \omega_2^2 q_2^{(2)} = &-d_2 D_0 q_2^{(0)} - 2D_0D_1 q_2^{(1)} - D_1^2 q_2^{(0)} - 2D_0D_2 q_2^{(0)}\\
&+ 2c_9 q_1^{(0)} q_1^{(1)} + c_5 q_1^{(0)^2} q_2^{(0)} + c_{13} q_2^{(0)^3} + 2c_{10} q_2^{(0)} q_2^{(1)}\\
&+ c_2 q_1^{(1)} q_3^{(0)} + c_{12} q_1^{(0)} q_2^{(0)} q_3^{(0)} + c_{14} q_2^{(0)} q_3^{(0)^3}\\
&+ c_2 q_1^{(0)} q_3^{(1)} + 2c_{11} q_3^{(0)} q_3^{(1)},
\end{aligned}$$

$$\begin{aligned}
D_0^2 q_3^{(2)} + \omega_3^2 q_3^{(2)} = &-d_3 D_0 q_3^{(0)} - 2D_0D_1 q_3^{(1)} - D_1^2 q_3^{(0)}\\
&- 2D_0D_2 q_3^{(0)} + c_{16} q_1^{(0)^3} + c_2 q_1^{(1)} q_2^{(0)}\\
&+ c_8 q_1^{(0)} q_2^{(0)^2} + c_2 q_1^{(0)} q_2^{(1)} + c_6 q_1^{(0)^2} q_3^{(0)}\\
&+ c_{14} q_2^{(1)^2} q_3^{(0)} + c_{15} q_2^{(1)} q_3^{(0)} + c_{18} q_1^{(0)} q_3^{(0)^2}\\
&+ c_{17} q_3^{(0)^3} + c_{15} q_2^{(0)} q_3^{(1)} + c_{20} p e^{i\Omega T_0},
\end{aligned} \tag{33}$$

where $D_i() = \partial()/\partial(T_i)$, $D_{ij}() = \partial^2()/\partial(T_i)\partial(T_j)$ $(i, j = 0,1,2)$ and the tilde has been omitted for simplicity.

The solution to the first-order perturbation Eq. (31) is:

$$q_i^{(0)} = A_i(T_1,T_2)e^{i\omega_i T_0} + c.c. \quad i = 1,2,3. \tag{34}$$

where *c.c.* stands for the complex conjugate of the preceding terms and $A_i$ are the unknown complex-valued functions. In order to investigate the system response under internal and external resonance conditions, three detuning parameters $\sigma_i$ are introduced:

$$\Omega = \omega_1 + \varepsilon^2\sigma_1, \quad \omega_2 = 2\omega_1 + \varepsilon\sigma_2, \quad \omega_3 = 3\omega_1 + \varepsilon^2\sigma_3. \tag{35}$$

Replacing the first-order solution Eq. (34) into Eq. (32), solving the $\varepsilon^2$-order perturbation equations and considering Eqs (35):

$$q_1^{(1)} = -\frac{c_1 A_1 A_2}{2\omega_1\omega_2 + \omega_2^2} e^{iT_0(\omega_1+\omega_2)} - \frac{c_2 A_2 A_3}{(\omega_2+\omega_3)^2 - \omega_1^2} e^{iT_0(\omega_2+\omega_3)} + c.c,$$

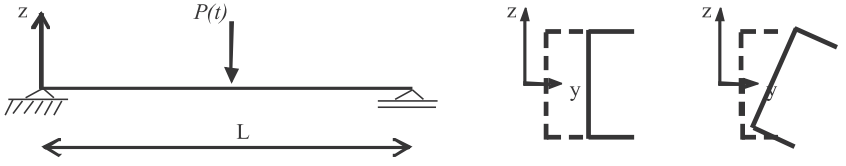


**Fig. 2.** Simply-supported C-beam and midspan section displacements of the fundamentals eigenfunctions.

$$q_2^{(1)} = -\frac{c_{10}A_2^2}{3\omega_2^2}e^{2iT_0\omega_2} - \frac{c_2A_1A_3}{(\omega_1+\omega_3)^2-\omega_2^2}e^{iT_0(\omega_1+\omega_3)} + \frac{c_{11}A_3^2}{\omega_2^2-4\omega_3^2}e^{2iT_0\omega_3} + \frac{2c_9A_1\bar{A}_1}{\omega_2^2} + \frac{2c_{10}A_2\bar{A}_2}{\omega_2^2} + \frac{2c_{11}A_3\bar{A}_3}{\omega_2^2} + c.c, \tag{36}$$

$$q_3^{(1)} = \frac{c_2A_1A_2}{\omega_3^2-(\omega_1-\omega_2)^2}e^{iT_0(\omega_1-\omega_2)} - \frac{c_{15}A_2\bar{A}_3}{\omega_2^2-2\omega_2\omega_3}e^{iT_0(\omega_2-\omega_3)} - \frac{c_{15}A_2A_3}{2\omega_2\omega_3+\omega_2^2}e^{iT_0(\omega_2+\omega_3)} + c.c.$$

Finally, substituting Eqs. (34) and (36) into the $\varepsilon^3$-order perturbation Eq. (33), eliminating the secular terms, then using a reconstitution method [22] to return to true time $t$, and finally introducing a Cartesian coordinates Eq. (37), the following amplitude and phase equations are obtained:

$$A_k = \frac{1}{2}(p_k - iq_k)e^{iv_k} \quad k = 1,2,3. \tag{37}$$

$$p_1' = -\frac{d_1p_1}{2} - q_1\sigma_1 - \frac{c_1p_2q_1\sigma_2}{8\omega_1^2} + \frac{c_1p_1q_2\sigma_2}{8\omega_1^2} + \frac{c_2p_3q_2\sigma_2}{8\omega_1^2} - \frac{c_2p_2q_3\sigma_2}{8\omega_1^2} - \frac{b_1p_1^2q_1}{8\omega_1} + \frac{c_1p_2q_1}{4\omega_1} - \frac{b_3p_2^2q_1}{8\omega_1} + \frac{b_2p_1p_3q_1}{4\omega_1} - \frac{b_5p_3^2q_1}{8\omega_1} - \frac{b_1q_1^3}{8\omega_1} - \frac{c_1p_1q_2}{4\omega_1} + \frac{c_2p_3q_2}{4\omega_1} - \frac{b_4p_2p_3q_2}{4\omega_1} - \frac{b_3q_1q_2^2}{8\omega_1} - \frac{b_2p_1^2q_3}{8\omega_1} - \frac{c_2p_2q_3}{4\omega_1} + \frac{b_4p_2^2q_3}{8\omega_1} + \frac{b_2q_1^2q_3}{8\omega_1} - \frac{b_4q_2^2q_3}{8\omega_1} - \frac{b_5q_1q_3^2}{8\omega_1}, \tag{38}$$

$$p_2' = -\frac{d_2p_2}{2} - 2q_2\sigma_1 - \frac{c_9p_1q_1\sigma_2}{4\omega_2^2} + \frac{c_2p_3q_1\sigma_2}{8\omega_2^2} + \frac{c_2p_1q_3\sigma_2}{8\omega_2^2} - \frac{c_9p_1q_1}{2\omega_2} + \frac{c_2p_3q_1}{4\omega_2} - \frac{b_9p_2p_3q_1}{8\omega_2} - \frac{b_6p_1^2q_2}{8\omega_2} - \frac{b_7p_2^2q_2}{8\omega_2} + \frac{b_9p_1p_3q_2}{8\omega_2} - \frac{b_8p_3^2q_2}{8\omega_2} - \frac{b_6q_1^2q_2}{8\omega_2} - \frac{b_7q_2^3}{8\omega_2} - \frac{c_2p_1q_3}{4\omega_2} - \frac{b_9p_1p_2q_3}{8\omega_2} - \frac{b_9q_1q_2q_3}{8\omega_2} - \frac{b_8q_2q_3^2}{8\omega_2}, \tag{39}$$

$$p_3' = -\frac{d_3p_3}{2} - 3q_3\sigma_1 + q_3\sigma_3 + \frac{c_2p_2q_1\sigma_2}{8\omega_3^2} + \frac{c_2p_1q_2\sigma_2}{8\omega_3^2} - \frac{3b_{10}p_1^2q_1}{8\omega_3} - \frac{c_2p_2q_1}{4\omega_3} + \frac{b_{11}p_2^2q_1}{8\omega_3} + \frac{b_{10}q_1^3}{8\omega_3} - \frac{c_2p_1q_2}{4\omega_3} - \frac{b_{11}p_1p_2q_2}{4\omega_3} - \frac{b_{11}q_1q_2^2}{8\omega_3} - \frac{b_{12}p_1^2q_3}{8\omega_3} - \frac{b_{13}p_2^2q_3}{8\omega_3} - \frac{b_{14}p_3^2q_3}{8\omega_3} - \frac{b_{12}q_1^2q_3}{8\omega_3} - \frac{b_{13}q_2^2q_3}{8\omega_3} - \frac{b_{14}q_3^3}{8\omega_3}, \tag{40}$$

$$q_1' = -\frac{d_1p_1}{2} - p_1\sigma_1 - \frac{c_1p_1p_2\sigma_2}{8\omega_1^2} + \frac{c_2p_2p_3\sigma_2}{8\omega_1^2} - \frac{c_1q_1q_2\sigma_2}{8\omega_1^2} + \frac{c_2q_2q_3\sigma_2}{8\omega_1^2} + \frac{c_{19}p}{\omega_1} + \frac{b_1p_1^3}{8\omega_1} + \frac{c_1p_1p_2}{4\omega_1} + \frac{b_3p_1p_2^2}{8\omega_1} + \frac{b_2p_1^2p_3}{8\omega_1} + \frac{c_2p_2p_3}{4\omega_1} + \frac{b_4p_2^2p_3}{8\omega_1} - \frac{b_5p_1p_3^2}{8\omega_1} + \frac{b_1p_1q_1^2}{8\omega_1} - \frac{b_2p_3q_1^2}{8\omega_1} + \frac{c_1q_1q_2}{4\omega_1} + \frac{b_3p_1q_2^2}{8\omega_1} - \frac{b_4p_3q_2^2}{8\omega_1} + \frac{b_2q_1q_3}{4\omega_1} + \frac{c_2q_2q_3}{4\omega_1} + \frac{b_4p_2q_2q_3}{4\omega_1} + \frac{b_5p_1q_3^2}{8\omega_1}, \tag{41}$$

$$q_2' = -\frac{d_2q_2}{2} + 2p_2\sigma_1 + \frac{c_9p_1^2\sigma_2}{8\omega_2^2} + \frac{c_2p_1p_3\sigma_2}{8\omega_2^2} - \frac{c_9q_1^2\sigma_2}{8\omega_2^2} + \frac{c_2q_1q_3\sigma_2}{8\omega_2^2} + \frac{c_9p_1^2}{4\omega_2} + \frac{b_6p_1^2p_2}{8\omega_2} + \frac{b_7p_2^3}{8\omega_2} + \frac{c_2p_1p_3}{4\omega_2} + \frac{b_9p_1p_2p_3}{8\omega_2} + \frac{b_8p_2p_3^2}{8\omega_2} - \frac{c_9q_1^2}{4\omega_2} + \frac{b_6p_2q_1^2}{8\omega_2} + \frac{b_9p_3q_1q_2}{8\omega_2} + \frac{b_7p_2q_2^2}{8\omega_2} + \frac{c_2q_1q_3}{4\omega_2} - \frac{b_9p_2q_1q_3}{8\omega_2} + \frac{b_9p_1q_2q_3}{8\omega_2} + \frac{b_8p_2q_3^2}{8\omega_2}, \tag{42}$$

$$q_3' = -\frac{d_3q_3}{2} + 3p_3\sigma_1 - p_3\sigma_3 - \frac{c_2p_1p_2\sigma_2}{8\omega_3^2} + \frac{c_2q_1q_2\sigma_2}{8\omega_3^2} + \frac{b_{10}p_1^3}{8\omega_3} + \frac{c_2p_1p_2}{4\omega_3} + \frac{b_{11}p_1p_2^2}{8\omega_3} + \frac{b_{12}p_1^2p_3}{8\omega_3} + \frac{b_{13}p_2^2p_3}{8\omega_3} + \frac{b_{14}p_3^3}{8\omega_3} - \frac{3b_{10}p_1q_1^2}{8\omega_3} + \frac{b_{12}q_1^2p_3}{8\omega_3} - \frac{c_2q_1q_2}{4\omega_3} + \frac{b_{11}p_2q_1q_2}{4\omega_3} - \frac{b_{11}p_1q_2^2}{8\omega_3} + \frac{b_{13}q_2^2p_3}{8\omega_3} + \frac{b_{14}p_3q_3^2}{8\omega_3}, \tag{43}$$

where the prime indicates the derivative with respect to $T_1$.

## 7. Numerical results

In this section the effect of shear deformation on the non-linear coupling and resonant motions are investigated for a C-beam simply supported; the following geometrical and material characteristic are used: $L$ = 6 m, $h$ = 0.6 m, $b$ = 0.6 m, $e$ = 0.03 m. The analyzed material is graphite-epoxy whose properties are $E_1$ = 144 GPa, $E_2$ = 9.65 GPa, $G_{12}$ = 4.14 GPa, $G_{13}$ = 4.14 GPa, $G_{23}$ = 3.45 GPa, $\nu_{12}$ = 0.3, $\nu_{13}$ = 0.3, $\nu_{23}$ = 0.5. The present model is used to analyze the steady-state motion and its stability considering different resonance conditions, modal damping and lamination sequences. The equilibrium solutions of Eqs. (38)–(43) correspond to periodic motions of the beam. Steady-state solutions are determined by zeroing $p_i' = q_i' = 0$ the right-hand members of the modulation Eqs. (38)–(43) and solving the non-linear system. Stability analysis is then performed by analyzing the eigenvalues of the Jacobian matrix of the non-linear equations calculated at the fixed points. The coefficients of the discretized equations of motion Eq. (29) are listed in Tables 1 and 2, denoting as *SS* and *WS* the values corresponding to the beam formulation with and without shear deformation.

The solution of the linear free dynamic problem gives the following first three eigenvalues for the sequence of lamination {0/0/0/0}:

$$\omega_1 = 214 \text{ rad/s}, \quad \omega_2 = 444 \text{ rad/s}, \quad \omega_3 = 666 \text{ rad/s},$$

and for the sequence of lamination {0/90/90/0}:

$$\omega_1 = 166 \text{ rad/s}, \quad \omega_2 = 356 \text{ rad/s}, \quad \omega_3 = 600 \text{ rad/s},$$

where $\omega_1$ and $\omega_3$ correspond to the flexural–torsional modes, while $\omega_2$ correspond to the uncouple lateral mode.

Now, the frequency–response curves (FRCs) of simply supported composite beams considering and neglecting shear deformation are presented. The modal amplitude curves $a_i$ are obtained in function of the external detuning parameter $\sigma_1$. The amplitudes $a_1$, $a_2$ and $a_3$ are obtained by means of the following expression:

$$a_i = \sqrt{p_i^2 + q_i^2} \quad i = 1,2,3. \tag{44}$$

Figs. 3 and 4 show the FRCs for a lamination sequences {0/90/90/0} and {0/0/0/0}, respectively. Next in the figures, solid (dashed) lines denote stable (unstable) equilibrium solutions and thin solid lines denote unstable foci. In this first case, the forcing amplitude

**Table 1**
Coefficients of the non-dimensional discretized equations of motion, lamination {0/0/0/0}.

| *Model* | $c_1$ | $c_2$ | $c_3$ | $c_4$ | $c_5$ | $c_6$ | $c_7$ |
|---|---|---|---|---|---|---|---|
| *SS* | 23134.1 | −38059.0 | −12549.1 | 51358.0 | −2057.4 | −93052.5 | 58212.7 |
| *WS* | 38355.6 | 125522.9 | −14873.7 | 3427.8 | −6223.4 | −49342.7 | −56520.8 |
| | $c_8$ | $c_9$ | $c_{10}$ | $c_{11}$ | $c_{12}$ | $c_{13}$ | $c_{14}$ |
| *SS* | 3375.58 | 11569.2 | 322.56 | 31345.8 | 6752.41 | −0.61 | 0.0 |
| *WS* | −9478.1 | 19181.7 | 1232.7 | 149395.4 | −18959.9 | −3.65 | 0.0 |
| | $c_{15}$ | $c_{16}$ | $c_{17}$ | $c_{18}$ | $c_{19}$ | $c_{20}$ | |
| *SS* | 62660.6 | 19398.2 | −87918.5 | 154026.0 | −0.00517 | −0.00651 | |
| *WS* | 298655.3 | −18835.5 | 63522.1 | 10280.9 | −0.00351 | 0.063536 | |

**Table 2**
Coefficients of the non-dimensional discretized equations of motion, lamination {0/90/90/0}.

| *Model* | $c_1$ | $c_2$ | $c_3$ | $c_4$ | $c_5$ | $c_6$ | $c_7$ |
|---|---|---|---|---|---|---|---|
| *SS* | 15189.6 | 29711.9 | −7174.8 | −24856.2 | −1748.6 | −48080.1 | −31810.8 |
| *WS* | 20484.1 | −67201.3 | −7949.9 | −1804.02 | −3330.1 | −26486.1 | 30263.7 |
| | $c_8$ | $c_9$ | $c_{10}$ | $c_{11}$ | $c_{12}$ | $c_{13}$ | $c_{14}$ |
| *SS* | −2806.7 | 7596.26 | 299.79 | 28232.1 | −5614.5 | −0.683 | 0.0 |
| *WS* | 5077.6 | 10244.1 | 660.7 | 80110.2 | 10157.3 | −1.959 | |
| | $c_{15}$ | $c_{16}$ | $c_{17}$ | $c_{18}$ | $c_{19}$ | $c_{20}$ | |
| *SS* | 56436.8 | −10600.5 | −39607.2 | −74546.6 | 0.00456 | −0.06504 | |
| *WS* | 160147.7 | 10085.3 | 34050.7 | −5410.7 | −0.00354 | −0.0635 | |

is $p = 250$, modal damping $d_1 = d_2 = d_3 = 0.1$ and the internal detuning parameters $\sigma_2 = 0.04$ and $\sigma_3 = 4$. It can be observed from the figures that the curves are composed by saddle-node and Hopf bifurcations, denoted as *SN* and *H*, respectively. As $\sigma_1$ increases from a small value, the solution increases in amplitude and is stable until a saddle-node bifurcation occurs ($SN_1$). Then the response jumps to another branch of stable equilibrium solutions (jump effect), depending on the initial conditions. Increasing $\sigma_1$, the amplitude decreases until the stable equilibrium solution loses stability via a Hopf bifurcation at $H_1$ and regains its stability via a reverse Hopf bifurcation at $H_2$. Then for $\sigma_1$ larger than the perfect external resonant condition, an approximated symmetric solution is observed in Fig. 3. For $\sigma_1 > H_2$ the stable solution grows again in amplitude until it arrives to a saddle-node bifurcation $SN_3$, resulting in a jump of the response to another solution branch. The new stable branch is left bounded by a saddle-node bifurcation $SN_4$. Comparing the three modal amplitude curves, the highest values of $a_i$ correspond to the first mode which is directly excited by the external load. The same behavior is observed in Fig. 4 for the lamination sequence {0/0/0/0}, but only for the case of the formulation with shear deformation (black curves). Conversely, when $\sigma_1 > 0$ the response obtained disregarding shear deformation is rather different (red curves). In fact, the theory without shear effect predicts a stable periodic solution for $\sigma_1$ larger than $H_2$, while the shear model predicts the existence an unstable branch with the possibility of jump amplitude effect. In both laminations analyzed, Figs. 3 and 4, the vibration amplitudes are lower when the shear deformation is neglected; this effect is larger for the sequence of lamination {0/0/0/0}. For example, the difference can reach about the 60% in the larger amplitude of the second mode. In the case of the lamination sequence {0/90/90/0}, the larger difference between both models (black and red curves) is about 37% in the third mode.

As it is known, the vibration amplitudes increase when the damping values are decreased; so, in the second case we want to establish the influence of the modal damping on the FRCs is analyzed for the lamination {0/0/0/0}. Fig. 5 presents the FRCs computed for both models, considering $d_1 = d_2 = d_3 = 0.05$. In comparison with the previous case (Fig. 4), it can be noted that the vibration amplitudes are larger (as expected) and the shear effect is more noticeable in the second mode. For example, the difference between the curves can reach about the 69%, which represents an increase of 9% in comparison with the previous case. Another discrepancy observed in Fig. 5 is when $\sigma_1 \cong 0$, the shear undeformable response (red curve) presents an unstable periodic solution (dashed lines) between the Hopf bifurcation $H_1$ and $H_2$, which is not present in the response with the shear theory (black curve). Investigating the nature of the dynamic solutions in this region, would demand a continuation analysis following the quasiperiodic response of the beam (limit cycles) that could be born from the Hopf bifurcations. For the sake of brevity, this analysis was not carried out in this work.

In the last case, Figs. 6 and 7 show the influence of the internal detuning parameters $\sigma_3 = 0.04$ on the FRCs, considering the modal damping $d_i = 0.1$ and 0.05, respectively. As can be noted from the figures, the response presents three peaks in amplitude corresponding to each resonance case. The curves are qualitatively similar; however, the influence of shear deformation is larger for lower modes. However, the difference between the amplitudes arrives at the saddle-node bifurcation denoted as $SN_5$ (central peak) can reach about the 53% for the third mode, when the damping is reduced to 0.05 (see Fig. 7). On the other hand, the unstable region below the curves bending either to the right or to the left (jump effect), are smaller when the shear deformation effect is neglected. Besides, this behavior is more noticeable for the first mode en both Figs. 6 and 7.

## 8. Summary and conclusions

In this paper the influence of shear deformation on the nonlinear dynamic of thin-walled laminated composite beam is analyzed. A non-linear beam theory is formulated in the context of large displacements and rotations, through the adoption of a

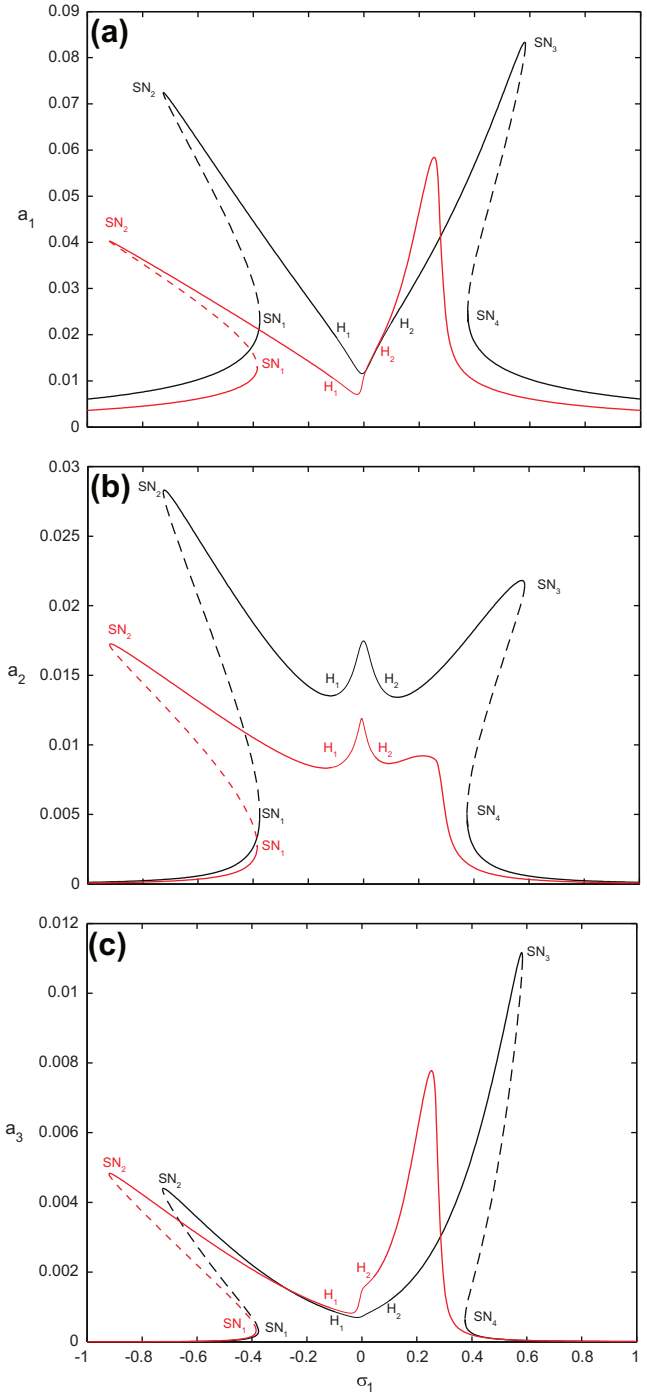


**Fig. 3.** Frequency–response curves for: (a) first, (b) second and (c) third modes, when $\sigma_3 = 4$, $d_i = 0.1$ and lamination {0/90/90/0}. Solid (dotted) lines denote stable (unstable) equilibrium solutions and thin solid lines denote unstable foci.

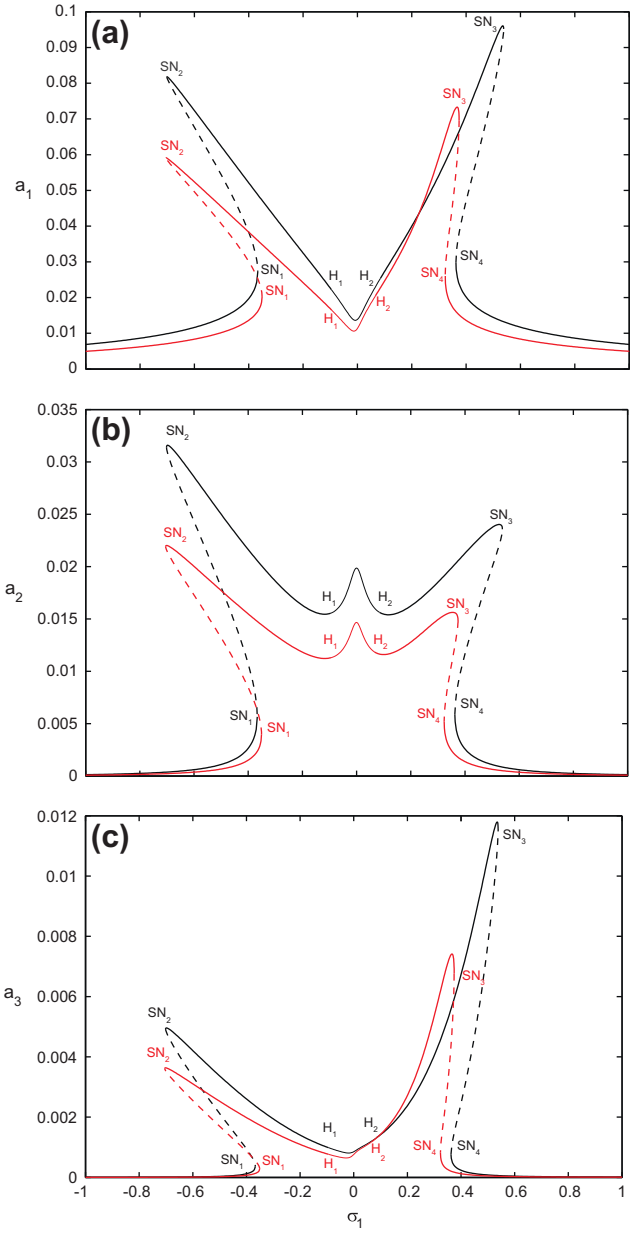


**Fig. 4.** Frequency–response curves for: (a) first, (b) second and (c) third modes, when $\sigma_3 = 4$, $d_i = 0.1$ and lamination {0/0/0/0}. Solid (dotted) lines denote stable (unstable) equilibrium solutions and thin solid lines denote unstable foci.

higher-order displacement field and takes into account shear flexibility (accounting for bending and warping shear). The response of a simply-supported beam under a vertical concentrated load to a primary resonant excitation of its first flexural–torsional mode is analyzed. The frequency of the second and third mode is approximately two and three times that of the first mode and hence a two-to-one and three-to-one internal resonance can be activated. With the method of multiple scales six first-order non-linear ordinary-differential equations describing the modulation of the amplitudes and phases are derived.

The influence of shear deformation on the non-linear coupling and resonant motions is noted in the numerical results and can be summarized as follows:

1. The amplitudes of the steady-state motions obtained by means of the shear undeformable theory are lower than the values obtained with the present shear model.
2. This effect is larger when the damping value is reduced.
3. The sizes of the unstable regions are influenced by the shear effect, when this effect is ignored the larger instability boundaries move down (jump behavior is also reduced). This behavior is originated by a decrease of the vibration amplitude values computed on the backbone of the resonance curves. As particular case, when $\sigma_3 = 4$ and lamination {0/0/0/0}, the discard of shear effect overestimates the stable region for $\sigma_1 > 0$.

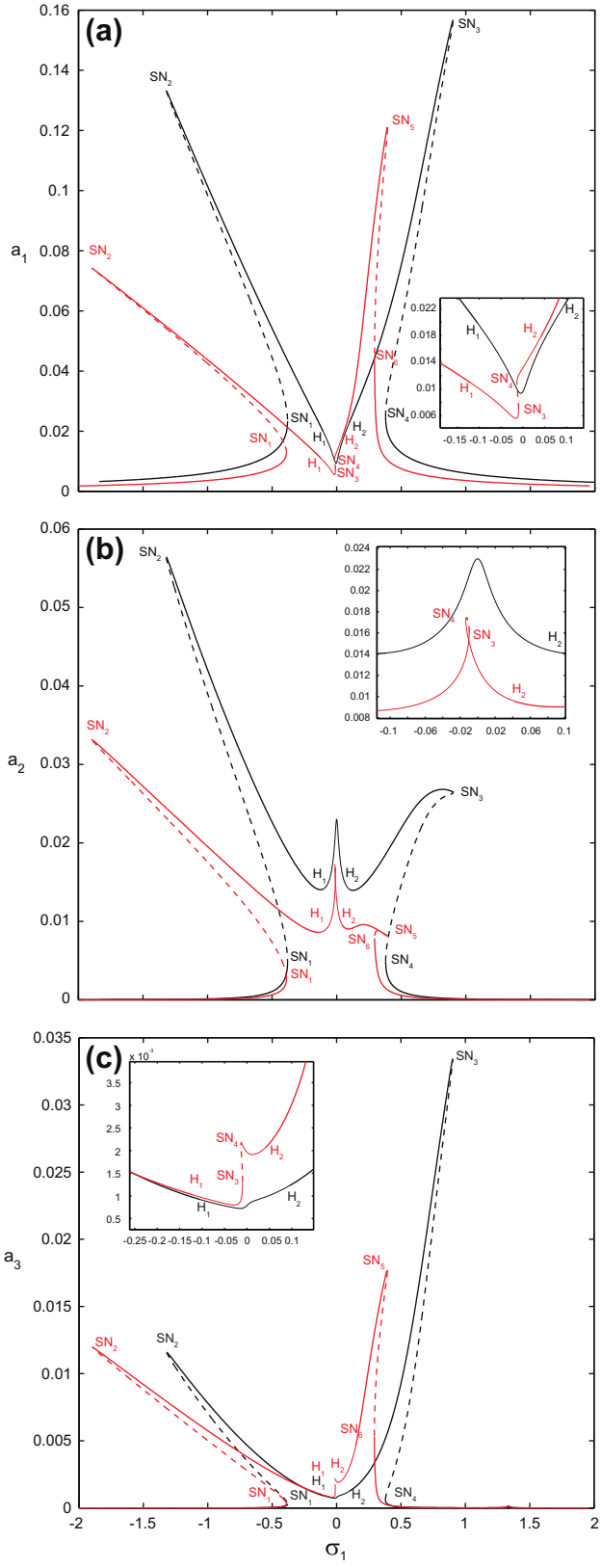


**Fig. 5.** Frequency–response curves for: (a) first, (b) second and (c) third modes, when $\sigma_3 = 4$, $d_i = 0.05$ and lamination {0/0/0/0}. Solid (dotted) lines denote stable (unstable) equilibrium solutions and thin solid lines denote unstable foci.

4. The lamination sequence plays an important role on the non-linear dynamic behavior of the beam. For example, the influence of shear deformation effect is more noticeable when the fibers are in a longitudinal direction, this is due to the lamination sequence {0/0/0/0} being stiffer behavior than {0/90/90/0}.
5. The non-linear dynamic behavior observed in the FRCs is also influenced by the interaction between modes. Selecting an internal detuning parameter of $\sigma_3 = 0.04$, it is found that the discrepancy in amplitude is larger for superior modes.
6. For this internal resonance condition, the FRCs exhibit a more complex behavior due to the presence of additional saddle-node and Hopf bifurcations in comparison with $\sigma_3 = 4$.

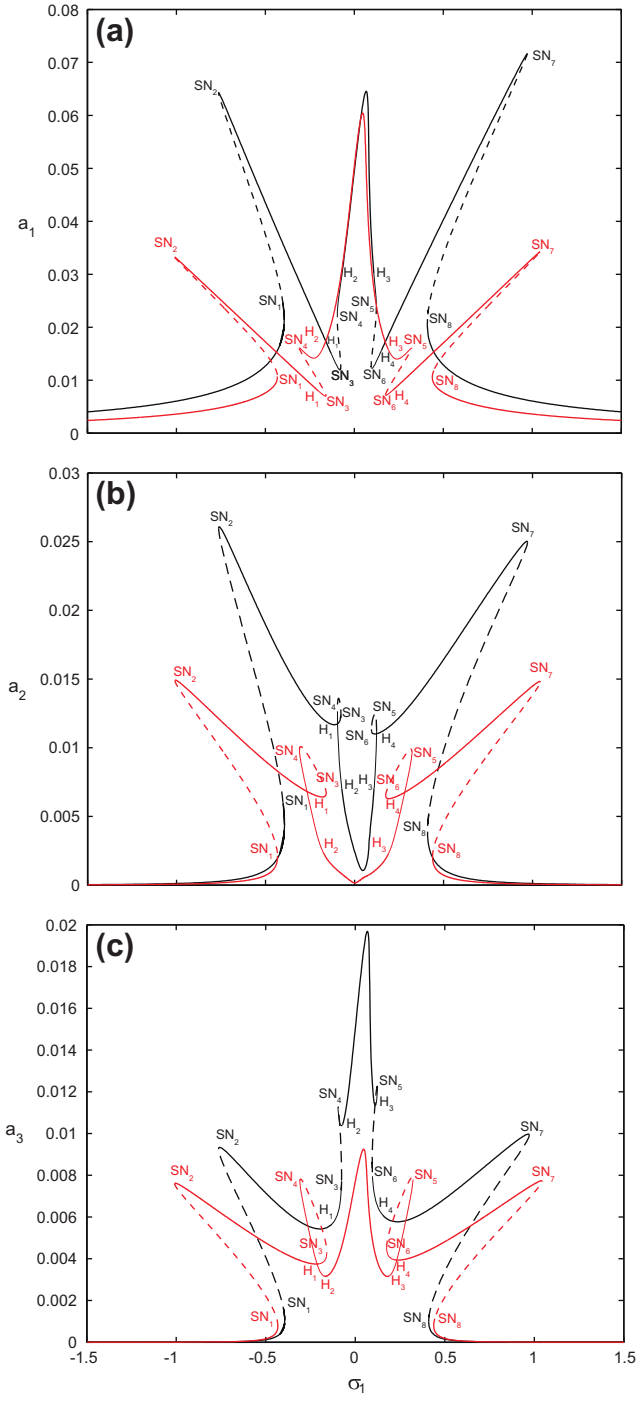


**Fig. 6.** Frequency–response curves for: (a) first, (b) second and (c) third modes, when $\sigma_3 = 0.04$, $d_i = 0.1$ and lamination {0/0/0/0}. Solid (dotted) lines denote stable (unstable) equilibrium solutions and thin solid lines denote unstable foci.

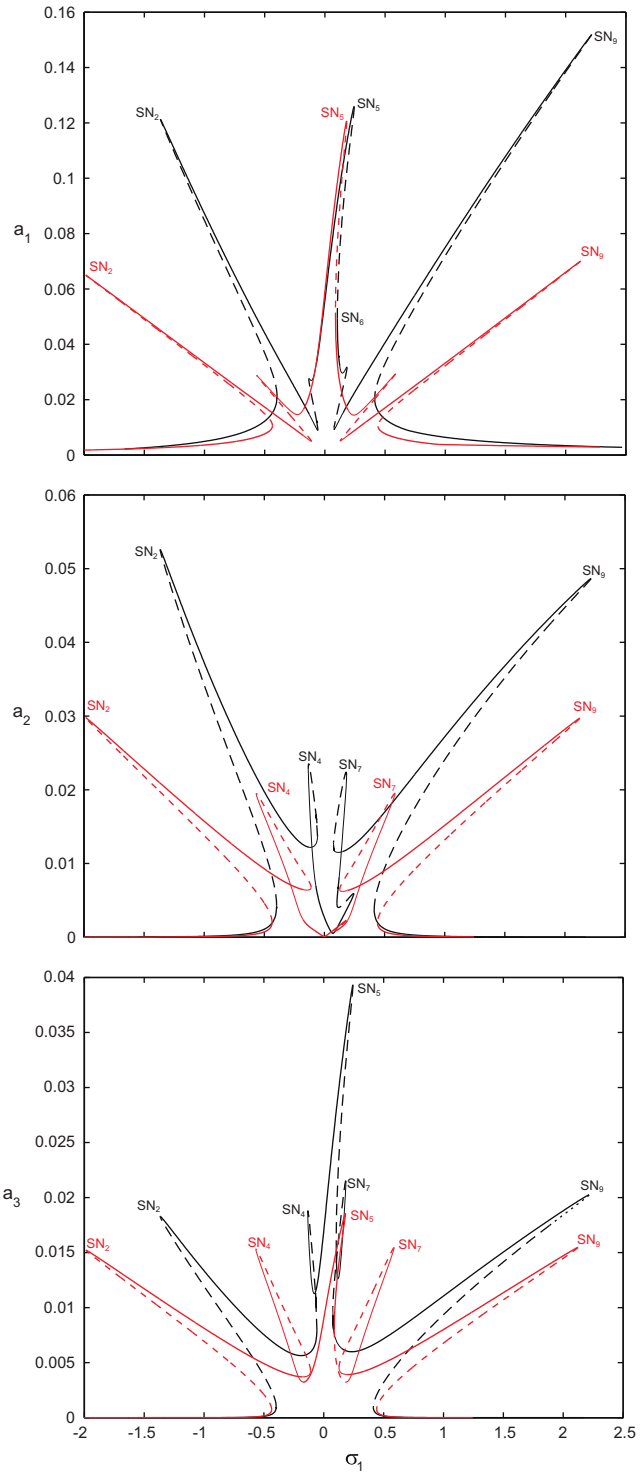


**Fig. 7.** Frequency–response curves for: first, second and third modes, when $\sigma_3 = 0.04$, $d_i = 0.05$ and for lamination {0/0/0/0}. Solid (dotted) lines denote stable (unstable) equilibrium solutions and thin solid lines denote unstable foci.

7. Finally, based on the non-linear dynamic response, it can be concluding that the discard of shear deformation effect results, inadvertently, in a less critical behavior in the frequency–response than in the case of its incorporation.

## Acknowledgments

The present study was sponsored by Secretaría de Ciencia y Tecnología, Universidad Tecnológica Nacional, and by CONICET.

## References

[1] Machado SP, Cortínez VH. Lateral buckling of thin-walled composite bisymmetric beams with prebuckling and shear deformation. Eng Struct 2005;27:1185–96.
[2] Machado SP. Interaction of combined loads on the lateral stability of thin-walled composite beams. Eng Struct 2010;32:3516–27.
[3] Sapkás A, Kollár LP. Lateral-torsional buckling of composite beams. Int J Solids Struct 2002;39:2939–63.
[4] Machado SP, Cortínez VH. Non-Linear model for stability of thin walled composite beams with shear deformation. Thin wall Struct 2005;43:1615–45.
[5] Sapountzakis EJ, Mokos VG. Shear deformation effect in nonlinear analysis of spatial beams. Eng Struct 2008;30:653–63.
[6] Machado SP, Filipich CP, Cortínez VH. Parametric vibration of thin-walled composite beams with shear deformation. J Sound Vib 2007;305:563–81.
[7] Machado SP, Cortínez VH. Dynamic stability of thin-walled composite beams under periodic transverse excitation. J Sound Vib 2009;321:220–41.
[8] Machado SP. Geometrically non-linear approximations on stability and free vibration of composite beams. Eng Struct 2007;29:3567–78.
[9] Nayfeh AH, Mook DT. Nonlinear oscillations. New York: Wiley; 1979.
[10] Nayfeh AH. Nonlinear interactions. New York: Wiley; 1996.
[11] Crespo da Silva MRM, Glynn CC. Nonlinear flexural–flexural–torsional dynamics of inextensional beams. I: Equations of motion. J Struct Mech 1978;6:437–48.
[12] Crespo da Silva MRM, Glynn CC. Nonlinear flexural–flexural–torsional dynamics of inextensional beams. II: Forced motions. J Struct Mech 1978;6:449–61.
[13] Luongo A, Rega G, Vestroni F. Non resonant non-planar free motions of inextensional non-compact beams. J Sound Vib 1989;134:73–86.
[14] Crespo da Silva MRM, Zaretzky CL. Nonlinear flexural–flexural–torsional interactions in beams including the effect of torsional dynamics – I: Primary resonance. Nonlinear Dynam 1994;5:3–23.
[15] Fonseca JR, Ribeiro P. Beam *p*-version finite element for geometrically non-linear vibrations in space. Comput Methods Appl Mech Eng 2006;195:905–24.
[16] Lopes Alonso R, Ribeiro P. Flexural and torsional non-linear free vibrations of beams using a *p*-version finite element. Comput Struct 2008;86:1189–97.
[17] Stoykov S, Ribeiro P. Nonlinear forced vibrations and static deformations of 3D beams with rectangular cross section: the influence of warping, shear deformation and longitudinal displacements. Int J Mech Sci 2010;52:1505–21.
[18] Luo SN, Ming FY, Yuan CZ. Non-linear vibration of composite beams with an arbitrary delamination. J Sound Vib 2004;271:535–45.
[19] Di Egidio A, Luongo A, Vestroni F. A non-linear model for the dynamics of open cross-section thin-walled beams – Part I: Formulation. Int J Nonlinear Mech 2003;38:1067–81.
[20] Di Egidio A, Luongo A, Vestroni F. A non-linear model for the dynamics of open cross-section thin-walled beams – Part II: Forced motion. Int J Nonlinear Mech 2003;38:1083–94.
[21] Nayfeh AH. Perturbation methods, pure and applied mathematics-A. New York: Wiley; 1973.
[22] Nayfeh AH, Balachandran B. Applied nonlinear dynamics: analytical computational and experimental methods. New York: Wiley; 1995.
[23] Barbero E. Introduction to composite material design. Philadelphia: Taylor and Francis Inc.; 1999.